Projection-Based Embedding with Projected Atomic Orbitals

Ádám B. Szirmai,[†,‡] Bence Hégely,[¶,§,‖] Attila Tajti,[*,†] Mihály Kállay,[¶,§,‖] and Péter G. Szalay[*,†]

†*Laboratory of Theoretical Chemistry, Institute of Chemistry, ELTE Eötvös Loránd University, P. O. Box 32, H-1518, Budapest 112, Hungary*

‡*György Hevesy Doctoral School, ELTE Eötvös Loránd University, Institute of Chemistry*

¶*Department of Physical Chemistry and Materials Science, Faculty of Chemical Technology and Biotechnology, Budapest University of Technology and Economics, Műegyetem rkp. 3., H-1111 Budapest, Hungary*

§*ELKH-BME Quantum Chemistry Research Group, Műegyetem rkp. 3., H-1111 Budapest, Hungary*

‖*MTA-BME Lendület Quantum Chemistry Research Group, Műegyetem rkp. 3., H-1111 Budapest, Hungary*

E-mail: attila.tajti@ttk.elte.hu; szalay@chem.elte.hu

Abstract

The projected atomic orbitals (PAO) technique is presented for the construction of virtual orbital spaces in projection-based embedding applications. The proposed straightforward procedure produces a set of virtual orbitals, which is used in the final, high-level calculation of the embedded active subsystem. The PAO scheme is demonstrated on intermolecular potentials of bimolecular complexes, in ground and excited

states, including Rydberg excitations. The results show the outstanding performance of the PbE embedding method with PAO virtual orbitals compared to those produced using common orbital localization techniques. The good agreement of the resulting PbE potential curves with those from high-level *ab initio* dimer calculations, also in diffuse basis sets, confirms that the PAO technique can be suggested for future applications of this type. The use of D3 dispersion corrections in such calculations is also proposed, supported by a superior accuracy over dispersion terms sourced from the effective fragment potential (EFP2) model.

Keywords: excited states, intermolecular interactions, embedding, PAOs

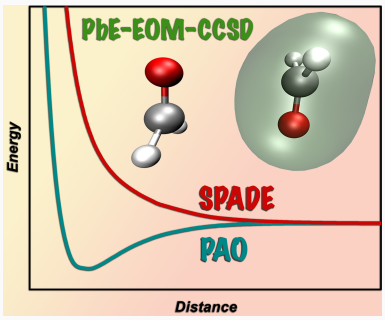

Embedding techniques[1] have emerged to be some of the most effective approaches to overcome the serious limitations of the applicability of high-level quantum chemistry methods due to the system size. This family of methods treat the relevant subsystem (reaction center, chromophore, etc.) at a higher level of theory while including the effect of the other parts in an approximate way, e.g., by using lower-level methods. Density Functional Theory (DFT) methods are ideal for embedding applications provided that the density can be distributed between the fragments and the functional form of the interactions allows a suitable definition of the embedding potential. Wave-function-in-DFT (WF-in-DFT) embedding approaches allow a treatment of the active fragment by advanced *ab initio* techniques, in particular by various formulations of Coupled Cluster theory,[2–4] also in excited electronic states[5–10] where the accuracy of these methods is often warranted even for a qualitatively correct description. In this type of embedding, top-down projector-based embedding $(\mathrm{PbE})^2$ strategies have the advantage of avoiding certain problematic non-additive terms[11] by using an orthogonal representation for the subsystems. A low-level calculation (usually at the DFT level) is performed first on the entire system, followed by a localization of the occupied orbitals on *a priori* defined sets of atoms (subsystems). This latter step is usually accomplished by using Pipek–Mezey localization,[12] intrinsic bond orbitals,[13] or the SPADE (Subsystem Projected AO DEcomposition)[14] technique and the orbital space belonging to the different fragments, which is then used to set up the embedding potential from the fragments' density, is defined by the position of the resulting localized orbitals. Subsequently, the orbitals of the active subsystem(s) are reoptimized under the influence of the embedding potential, applying the orthogonality constrain between the subsystems by level shifting,[2] solving the Huzinaga equation,[3] or by applying the projection scheme by Hoffmann et al.[15] The high-level correlated calculations on the active fragment are finally performed using the Fock matrix that results from the above procedure. Since only the electrons defining the density on the active fragment(s) are used in these calculations, a significant reduction of the cost of the calculation is achieved.

Nevertheless, the original formulations of PbE[2,3] leave the space of virtual orbitals intact, i.e., that of the original supersystem, which poses serious limitations on the applicability of the higher-level *ab initio* methods due to the unfavorable scaling of the computational cost

with the size of the virtual space. In addition, the untruncated virtual space tendentially leads to the appearance of artefactual low-lying charge transfer (CT) states,[16] often rendering the identification of local excited states impossible. Several approaches have been investigated to deal with this problem by truncating the virtual space in a reasonable way, including the absolutely localized embedding schemes of Chulhai and Goodpaster[4,6] that avoid the issue entirely by using monomer basis sets, or the basis set truncation method for PbE by Bennie et al[17] which relies on net Mulliken population criteria. Claudino and Mayhall developed a concentric virtual orbital localization technique[18] which has been used by Parravicini and Jagau in embedded excited state calculations.[8] Visscher and co-workers generalized the intrinsic atomic orbital approach[13] to molecular fragments,[19] constructing orthogonal localized orbitals by spanning the supersystem valence and virtual space[20] using reference fragment orbitals. Conventional MO-based localizations, such as Pipek-Mezey[12] and SPADE[14] can also be applied to the virtual space, and by assigning orbitals to the subsystems based on some selection criteria, those of the environment can be discarded.[21] We observed, however, that without any further adjustments, the resulting virtual space can be severely distorted compared to that of an isolated monomer.[16] The distortion can be reduced by extending the space by some environment orbitals that show the largest overlap with the atomic orbitals centered on the active subsystem. Nevertheless, the effective construction of appropriate virtual orbitals, especially if diffuse basis functions are present, remains a challenge in PbE applications. Improper virtual spaces can cause a drastic overestimation of the energy and result in nonphysically repulsive intermolecular potentials,[16] calling for a compelling remedy for this issue. In this letter, the use of projected atomic orbitals (PAOs) is suggested as an alternative for creating virtual orbitals localized on the active subsystem.

PAOs were first suggested by Boughton and Pulay[22] to define the virtual space in local correlation calculations. We suggest the implementation of this concept in PbE, relying on the use of the atomic orbitals centered on the active subsystem's atoms as the basis for the construction of a virtual space (the PAOs).

We define the projector of the occupied orbitals of the supersystem as

$$\mathbf{R} = \mathbf{C}_{\mathrm{occ}}\mathbf{C}_{\mathrm{occ}}^{\mathrm{T}}, \tag{1}$$

where $\mathbf{C}_{\mathrm{occ}}$ is the occupied orbital block of the MO coefficient matrix. The application of this projector leads to the PAOs

$$\mathbf{C}_{\mathrm{PAO}} = \mathbf{1} - \mathbf{RS}, \tag{2}$$

where $\mathbf{S}$ is the AO overlap matrix. Some of these PAOs can have negligible contribution to the virtual space of the active subsystem, furthermore, linear dependencies are present at this point. Truncations are therefore performed, first according to the norm of the PAOs obtained as

$$N_i = \sum_{\mu}^{\text{act.AOs}} (\mathbf{C}_{\mathrm{PAO}})_{i\mu} (\mathbf{S}\mathbf{C}_{\mathrm{PAO}})_{i\mu} \ , \tag{3}$$

where the indices μ and i label AOs of the active subsystem (act.AOs) and the PAOs, respectively. PAOs with N_i below an appropriately chosen threshold are discarded, and the rest are renormalized, producing a new set of PAOs, $\mathbf{C}'_{\mathrm{PAO}}$.

To eliminate linear dependencies from this set, a second truncation step is introduced by screening the redundant PAOs via the diagonalization of their overlap matrix

$$\mathbf{S}_{\mathrm{PAO}} = (\mathbf{C}'_{\mathrm{PAO}})^{\mathrm{T}} \, \mathbf{S} \, \mathbf{C}'_{\mathrm{PAO}}, \tag{4}$$

so that only PAOs with an absolute value of their eigenvalue $|s_i|$ above a chosen truncation parameter are retained. The resulting set of linearly independent PAOs are finally used as the virtual orbital basis when solving the Huzinaga equation.[3] Details are given in Section S1.3 of the Supporting Information.

The generation of PAOs using the above scheme thus requires the definition of the atoms used for the construction of the PAOs, as well as two truncation parameters, one for the post-projection norm (N_i) and another for the tolerance of the overlap for redundant orbitals ($|s_i|$). This scheme has been implemented in the MRCC program code.[23,24]

We evaluate the effect of the virtual space truncation on the quality of the interaction potential energy curves, both in ground and excited states, for the stacked homodimers of formaldehyde [$(CH_2O)_2$] and pyrrole [$(Pyr)_2$], as well as for the cytosine-uracil complex [Cyt-Ura]. These test systems have been studied in a recent work,[16] and their structures are available in the Supporting Information. As reference, we use Coupled Cluster with Singles

and Doubles (CCSD)[25] and Equation-of-Motion Coupled Cluster with Singles and Doubles (EOM-CCSD)[26,27] calculations for the ground and excited states, respectively, corrected for the basis set superposition error (BSSE). For the excited states of the homodimers, a single reference curve is obtained by averaging the energies of the two interacting states, that is, by removing the excitonic coupling. The same wave function methods are employed in the WF-in-DFT type PbE, with the low-level DFT calculations using the Perdew–Burke–Ernzerhof (PBE) functional.[28] To make meaningful comparisons to the reference, the interaction energy has to be augmented by a dispersion correction,[16,21] for which the D3 dispersion correction by Grimme was chosen,[29] as justified later. All calculations have been performed by the MRCC suite of codes.[23,24] Further details of the test calculations can be found in the Supporting Information.

On panel A of Figure 1, the ground state potential energy curves for the $[(CH_2O)_2]$ dimer are shown, calculated with four different virtual spaces: the full virtual space, one localized with the SPADE procedure, the latter extended by two additional virtual orbitals (denoted as "ext. SPADE"), as well as with the space produced with the PAO scheme. It is clearly seen that while with the full valence space the interaction energy is slightly overestimated, the SPADE localization results in a far too small interaction energy. Adding the two environment orbitals with the largest overlap with the AOs of the active subsystem improves the results considerably, while with PAO virtual orbitals an almost perfect curve is obtained.

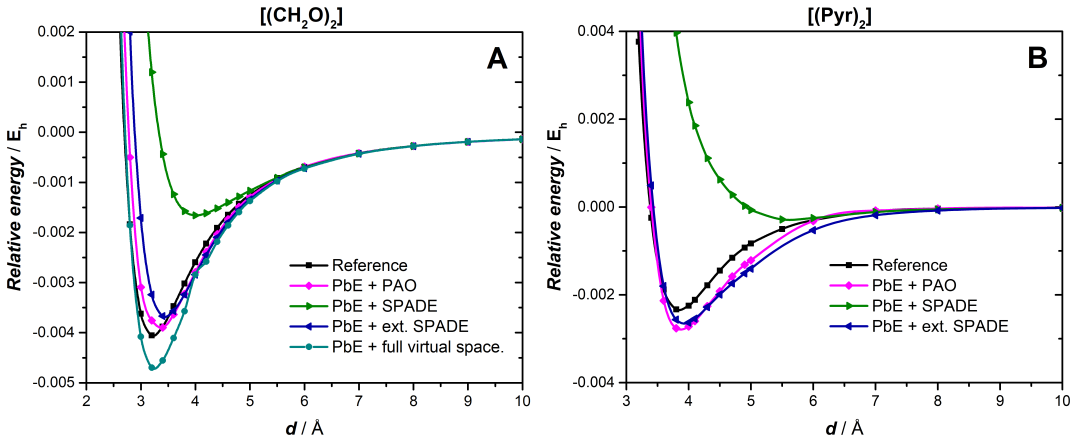

Figure 1: CCSD ground-state interaction energies (in atomic units) of the $[(CH_2O)_2]$ (Panel A, $N = 0.05$, $s = 10^{-3}$) and $[(Pyr)_2]$ (Panel B, $N = 0.05$, $s = 9 \cdot 10^{-5}$) homodimer complexes as functions of the intermolecular separation d, evaluated in the aug-cc-pVDZ basis.

Similar conclusions can be drawn in the case of $[(Pyr)_2]$ (Panel B of Figure 1), where again the PAO virtual space gives the best potential energy curves. (Note that for this system "ext. SPADE" includes seven additional orbitals.)

For the Rydberg type excited states obtained in the diffuse aug-cc-pVDZ basis (Figure 2), the SPADE localization results in repulsive interaction curves. This is the consequence of, as discussed in Ref. 16, the requirement that for the correct description of the Rydberg states the virtual orbitals have to extend to the space where the other fragment resides. However, the standard localization procedures cut off this part of the virtual basis, deteriorating the wave function more and more with decreasing distance between the fragments. We have called this effect the *reverse BSSE* in Ref. 16. As evident from Panel A of Figure 2, the extension of the virtual space by the most overlapping orbitals of the environment does not solve the problem, the respective potential curve is still repulsive. On the other hand, the use of a PAO virtual space provides a solution here since the diffuse functions of the active fragments are retained in the basis, irrespective of their overlap with the other fragment. In the case of $[(CH_2O)_2]$ (Panel A), we again get a nearly perfect curve with PAOs, while the improvement is also apparent for the two investigated Rydberg states of $[(Pyr)_2]$ (Panels B and C). Note that in the latter system, CT contributions become significant in the reference wave function at short distances, thus a good agreement of PbE and the reference is only expected at separations above 4 Å.[16]

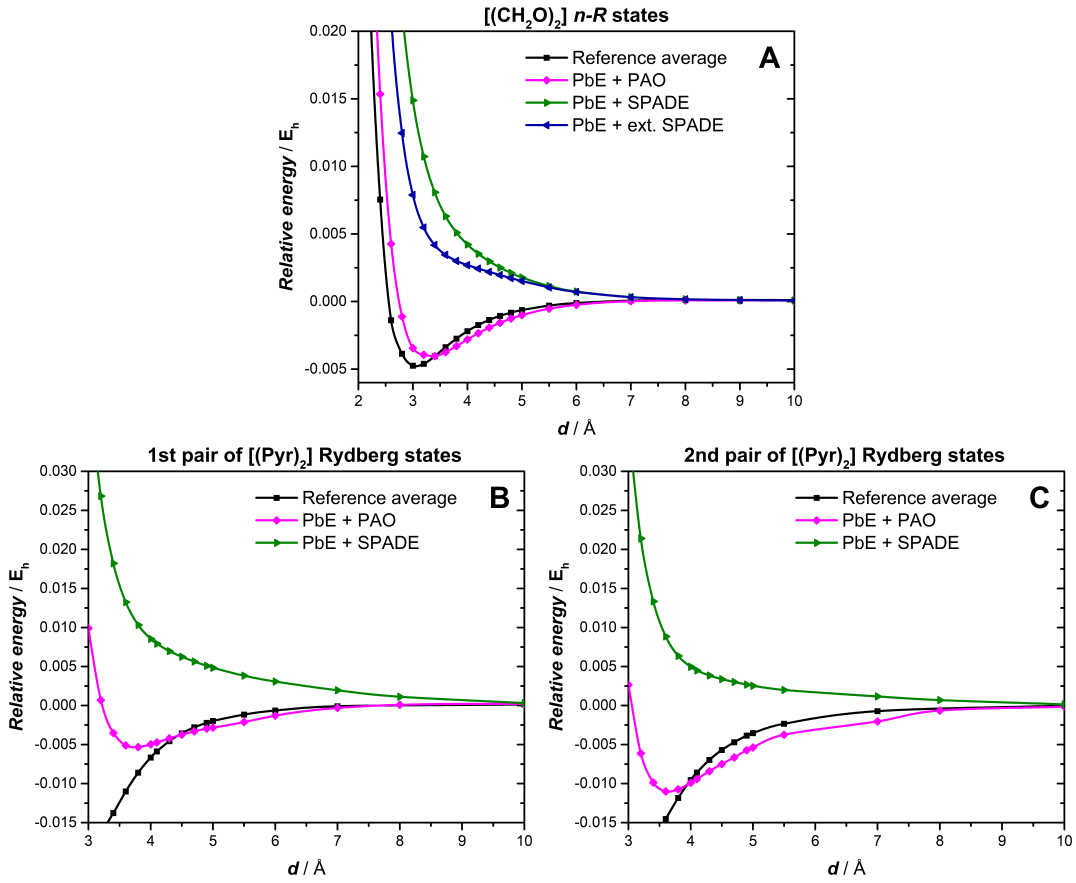

Figure 2: EOM-CCSD averaged interaction energies of different Rydberg excited state pairs in the $[(CH_2O)_2]$ (Panel A, $N = 0.05$, $s = 10^{-3}$) and $[(Pyr)_2]$ (Panels B and C, $N = 0.05$, $s = 9 \cdot 10^{-5}$) homodimer complexes as functions of the intermolecular separation d, evaluated in the aug-cc-pVDZ basis.

This also applies to the $\sigma - \pi^*$ and $\pi - \pi^*$ valence excited states of $[(CH_2O)_2]$ calculated in the aug-cc-pVDZ basis, shown on panels A and B of Figure 3. Nevertheless, only the curves obtained with PAO virtual orbitals are attractive, fixing the qualitatively wrong repulsive behavior of the ones based on the SPADE localization. Since here the reference states are more strongly affected by the problem of crossing CT states,[16] their agreement with PbE is less good than in the examples above.

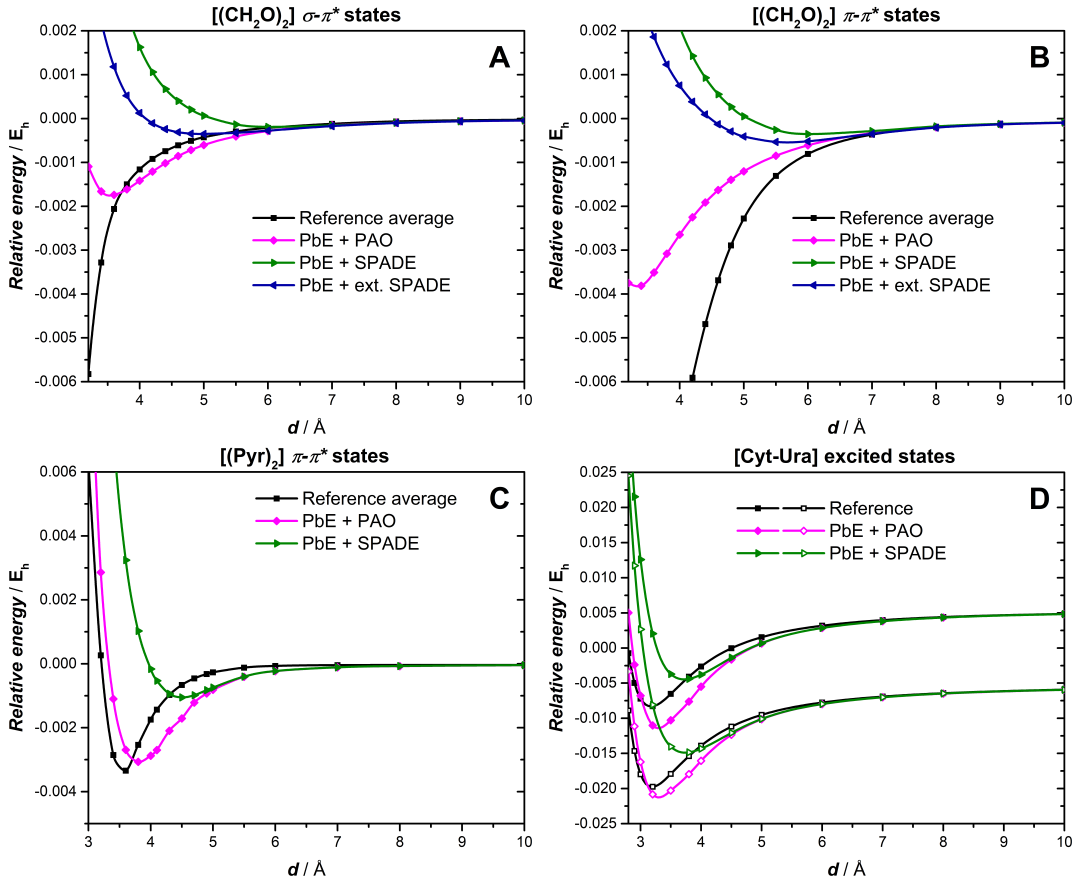

Figure 3: EOM-CCSD averaged interaction energies of different valence excited state pairs: $\sigma - \pi^*$ and $\pi - \pi^*$ states of the $[(CH_2O)_2]$ complex (Panels A and B, aug-cc-pVDZ basis, $N = 0.05$, $s = 10^{-3}$) and $\pi - \pi^*$ excited states of the $[(Pyr)_2]$ homodimer complex (Panel C, cc-pVDZ basis, $N = 0.05$, $s = 10^{-3}$), and the $\pi - \pi^*$ excited states of the [Cyt-Ura] complex (Panel D, no averaging, cc-pVDZ basis, $N = 0.05$, $s = 10^{-3}$) as functions of the intermolecular separation d.

The effect of disturbing CT contributions can be eliminated with the use of basis sets that do not include diffuse functions, with the disadvantage of less accurate interaction energies. On panel C of Figure 3, the curves obtained for the π-π^* state of $[(Pyr)_2]$ with the cc-pVDZ basis set are shown, and the PAO technique is indeed found to perform excellently in this non-diffuse basis. Note, however, that the truncation based on the SPADE localization also gives an attractive, although less accurate potential curve for this state. This proper behavior can be explained by the small overlap of the active fragment orbitals with the environment, even at short distances.

Also for the pair of $\pi - \pi^*$ excited states of the [Cyt-Ura] complex shown on Panel

D of Figure 3, this truncation method predicts bound configurations, but the interaction energy and the equilibrium distance are significantly under- and overestimated, respectively. Compared to these curves, the PAO approach brings a clear improvement yet again and a satisfactory agreement with the reference calculations. Note that in this example the interaction of the two states via excitonic couplings is also included in the embedding models using the scheme described in Ref. 16 (see the Supporting Information for more details).

Finally, a note on the dispersion correction used to correct the PbE potential curves in order to allow a comparison with the reference. In our previous study[16] on the ground state interaction curves, the use of dispersion sourced from the EFP2 model[30] was suggested, based on its better agreement with the respective term in Symmetry-Adapted Perturbation Theory (SAPT).[31,32] The D3 correction showed, in contrast, a considerable underestimation of this quantity. However, for the present results calculated with PbE and PAO virtual orbitals, the use of the D3 dispersion correction — with parameters chosen for the employed DFT functional — is found to be more appropriate. With the EFP2 dispersion term, the interaction energy is, as seen in Figure 4, severely overestimated. This is line with the finding of Szalewicz et al.[33] that in the case of DFT, the overall quality of the interaction energy curve is improved if the smaller D3 correction is used instead of the theoretically more accurate dispersion calculated by SAPT. On the other hand, in the case of a purely electrostatic embedding such as QM/MM, the electrostatic interaction needs to be augmented with the complete/entire dispersion, e.g., by EFP2 as suggested earlier in Ref. 16.

In summary, the results presented here show the superior performance of the PbE embedding method using PAOs for virtual orbitals. Not only are the calculations cheap (the same as the calculation on the bare fragment), but the potential curves follow the reference curves obtained for the supersystem nicely. This is true for both ground and excited states, including both valence and Rydberg type excitations. We have also confirmed the finding of Szalewicz[33] that the D3 is the appropriate dispersion correction to be used with DFT and we suggest its use also in WF-in-DFT embedding calculations.

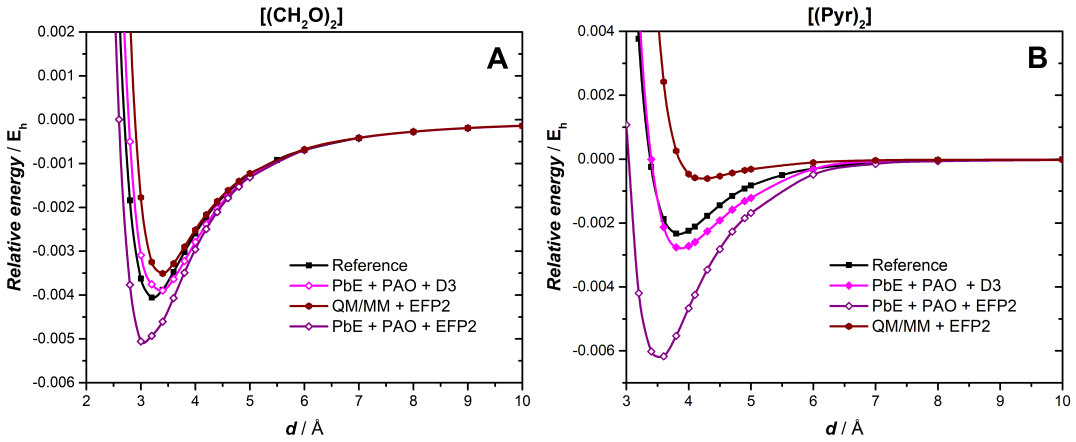

Figure 4: Comparison of the D3 and EFP2 dispersion corrections. Ground state CCSD interaction energy curves of the $[(CH_2O)_2]$ (Panel A, $N = 0.05$, $s = 10^{-3}$) and $[(Pyr)_2]$-(Panel B, $N = 0.05$, $s = 9 \cdot 10^{-5}$) complexes as functions of the intermolecular separation d, calculated by different methods with aug-cc-pVDZ basis. QM/MM and EFP2 data from Ref.[16]

Acknowledgments

This work has been supported by the National Research, Innovation and Development Fund (NKFIA) of Hungary Grant No. 142634 and KKP126451. The authors thank Bónis Barcza for discussions and providing the QM/MM and EFP2 numbers.

Data availability statement

The data supporting the findings of this study are available in the supplementary material.

Conflict of interest

The authors declare no conflict of interest.

Supporting Information

Details of the calculations, structures of the monomers and complexes evaluated in this study.

References

1. Goez, A.; Neugebauer, J. In *Frontiers of Quantum Chemistry*; Wójcik, M. J., Nakatsuji, H., Kirtman, B., Ozaki, Y., Eds.; Springer Singapore: Singapore, 2018; pp 139–179.

2. Manby, F. R.; Stella, M.; Goodpaster, J. D.; Miller, T. F. I. A Simple, Exact Density-Functional-Theory Embedding Scheme. *Journal of Chemical Theory and Computation* **2012**, *8*, 2564–2568, PMID: 22904692.

3. Hégely, B.; Nagy, P. R.; Ferenczy, G. G.; Kállay, M. Exact density functional and wave function embedding schemes based on orbital localization. *The Journal of Chemical Physics* **2016**, *145*, 064107.

4. Chulhai, D. V.; Goodpaster, J. D. Improved Accuracy and Efficiency in Quantum Embedding through Absolute Localization. *Journal of Chemical Theory and Computation* **2017**, *13*, 1503–1508.

5. Bennie, S. J.; Curchod, B. F. E.; Manby, F. R.; Glowacki, D. R. Pushing the Limits of EOM-CCSD with Projector-Based Embedding for Excitation Energies. *The Journal of Physical Chemistry Letters* **2017**, *8*, 5559–5565, PMID: 29076727.

6. Wen, X.; Graham, D. S.; Chulhai, D. V.; Goodpaster, J. D. Absolutely Localized Projection-Based Embedding for Excited States. *Journal of Chemical Theory and Computation* **2020**, *16*, 385–398, PMID: 31769981.

7. Zech, A.; Ricardi, N.; Prager, S.; Dreuw, A.; Wesolowski, T. A. Benchmark of Excitation Energy Shifts from Frozen-Density Embedding Theory: Introduction of a Density-Overlap-Based Applicability Threshold. *Journal of Chemical Theory and Computation* **2018**, *14*, 4028–4040, PMID: 29906111.

8. Parravicini, V.; Jagau, T.-C. Embedded equation-of-motion coupled-cluster theory for electronic excitation, ionisation, electron attachment, and electronic resonances. *Molecular Physics* **2021**, *119*, e1943029.

9. Hégely, B.; Szirmai, Á. B.; Mester, D.; Tajti, A.; Szalay, P. G.; Kállay, M. Performance of Multilevel Methods for Excited States. *The Journal of Physical Chemistry A* **2022**, *126*, 6548–6557, PMID: 36095318.

10. Gomes, A. S. P.; Jacob, C. R.; Visscher, L. Calculation of local excitations in large systems by embedding wave-function theory in density-functional theory. *PHYSICAL CHEMISTRY CHEMICAL PHYSICS* **2008**, *10*, 5353–5362.

11. Jacob, C. R.; Neugebauer, J. Subsystem density-functional theory. *WIREs Computational Molecular Science* **2014**, *4*, 325–362.

12. Pipek, J.; Mezey, P. A Fast Intrinsic Localization Procedure Applicable For Abinitio And Semiempirical Linear Combination Of Atomic Orbital Wave-Functions. *J. Chem. Phys.* **1989**, *90*, 4916–4926.

13. Knizia, G. Intrinsic Atomic Orbitals: An Unbiased Bridge between Quantum Theory and Chemical Concepts. *Journal of Chemical Theory and Computation* **2013**, *9*, 4834–4843.

14. Claudino, D.; Mayhall, N. J. Automatic Partition of Orbital Spaces Based on Singular Value Decomposition in the Context of Embedding Theories. *Journal of Chemical Theory and Computation* **2019**, *15*, 1053–1064.

15. Khait, Y. G.; Hoffmann, M. R. In *Annual Reports in Computational Chemistry*; Wheeler, R. A., Ed.; Annual Reports in Computational Chemistry; Elsevier, 2012; Vol. 8; pp 53–70.

16. Barcza, B.; Szirmai, A. B.; Tajti, A.; Stanton, J. F.; Szalay, P. G. Benchmarking Aspects of Ab Initio Fragment Models for Accurate Excimer Potential Energy Surfaces. *Journal of Chemical Theory and Computation* **2023**, *19*, 3580–3600.

17. Bennie, S. J.; Stella, M.; Miller, I., Thomas F.; Manby, F. R. Accelerating wavefunction in density-functional-theory embedding by truncating the active basis set. *The Journal of Chemical Physics* **2015**, *143*, 024105.

18. Claudino, D.; Mayhall, N. J. Simple and Efficient Truncation of Virtual Spaces in Embedded Wave Functions via Concentric Localization. *The Journal Chemical Theory and Computations* **2019**, *15*, 6085 – 6096.

19. Senjean, B.; Sen, S.; Repisky, M.; Knizia, G.; Visscher, L. Generalization of Intrinsic Orbitals to Kramers-Paired Quaternion Spinors, Molecular Fragments, and Valence Virtual Spinors. *Journal of Chemical Theory and Computation* **2021**, *17*, 1337–1354.

20. Sen, S.; Senjean, B.; Visscher, L. Characterization of excited states in time-dependent density functional theory using localized molecular orbitals. *The Journal of Chemical Physics* **2023**, *158*, 054115.

21. Barcza, B.; Szirmai, Á. B.; Szántó, K. J.; Tajti, A.; Szalay, P. G. Comparison of approximate intermolecular potentials for ab initio fragment calculations on medium sized N-heterocycles. *Journal of Computational Chemistry* **2022**, *43*, 1079–1093.

22. Boughton, J. W.; Pulay, P. Comparison of the Boys and Pipek–Mezey localizations in the local correlation approach and automatic virtual basis selection. *Journal Of Computational Chemistry* **1993**, *14*, 736 – 740.

23. Kállay, M.; Nagy, P. R.; Mester, D.; Gyevi-Nagy, L.; Csóka, J.; Szabó, P. B.; Rolik, Z.; Samu, G.; Csontos, J.; Hégely, B.; Ganyecz, Á.; Ladjánszki, I.; Szegedy, L.; Ladóczki, B.; Petrov, K.; Farkas, M.; Mezei, P. D.; Horváth, R. A. MRCC, a quantum chemical program suite. See https://www.mrcc.hu/, Accessed December 1, 2023.

24. Kállay, M.; Nagy, P. R.; Mester, D.; Rolik, Z.; Samu, G.; Csontos, J.; Csóka, J.; Szabó, P. B.; Gyevi-Nagy, L.; Hégely, B.; Ladjánszki, I.; Szegedy, L.; Ladóczki, B.; Petrov, K.; Farkas, M.; Mezei, P. D.; Ganyecz, A. The MRCC program system: Accurate quantum chemistry from water to proteins. *The Journal of Chemical Physics* **2020**, *152*, 074107.

25. Bartlett, R. J.; Purvis III, G. D. Molecular Applications of Coupled Cluster and Many-Body Perturbation Methods. *Phys. Scr.* **1980**, *21*, 255–265.

26. Stanton, J. F.; Bartlett, R. J. The Equation of Motion Coupled-Cluster Method - A Systematic Biorthogonal Approach to Molecular-Excitation Energies, Transition-Probabilities, and Excited-State Properties. *J. Chem. Phys.* **1993**, *98*, 7029–7039.

27. Comeau, D. C.; Bartlett, R. J. The Equation-of-Motion Coupled-Cluster Method - Applications to Open-Shell and Closed-Shell Reference States. *Chem. Phys. Lett.* **1993**, *207*, 414–423.

28. Perdew, J. P.; Burke, K.; Ernzerhof, M. Generalized Gradient Approximation Made Simple. *Phys. Rev. Lett.* **1996**, *77*, 3865–3868.

29. Grimme, S.; Antony, J.; Ehrlich, S.; Krieg, H. A consistent and accurate ab initio parametrization of density functional dispersion correction (DFT-D) for the 94 elements H-Pu. *The Journal of Chemical Physics* **2010**, *132*, 154104.

30. Slipchenko, L. V.; Gordon, M. S.; Ruedenberg, K. Dispersion Interactions in QM/EFP. *The Journal of Physical Chemistry A* **2017**, *121*, 9495–9507.

31. Jeziorski, B.; Moszynski, R.; Szalewicz, K. Perturbation Theory Approach to Intermolecular Potential Energy Surfaces of van der Waals Complexes. *Chemical Reviews* **1994**, *94*, 1887–1930.

32. Szalewicz, K. Symmetry-adapted perturbation theory of intermolecular forces. *WIREs Computational Molecular Science* **2012**, *2*, 254–272.

33. Shahbaz, M.; Szalewicz, K. Do Semilocal Density-Functional Approximations Recover Dispersion Energies at Small Intermonomer Separations? *Physical Review Letters* **2018**, *121*, 113402.